Antifreeze Polyvinyl Alcohol Organohydrogel Sensors Containing Polypyrrole Nanowires SelfAssembled onto Graphene Oxide Nanoplatelets with High Electrical Conductivity and

RESEARCH ARTICLE

Antifreeze Polyvinyl Alcohol Organohydrogel Sensors Containing Polypyrrole Nanowires Self-Assembled onto Graphene Oxide Nanoplatelets with High Electrical Conductivity and Improved Mechanical Properties

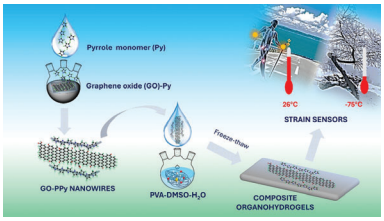

New organohydrogels based on polyvinyl alcohol/water/dimethylsulfoxide and containing polypyrrole nanowires-modified graphene oxide show antifreeze properties, retaining their flexibility at temperatures as low as −75 °C, and display high electrical conductivity and stable electrical response to cyclic deformation, allowing their application as movement sensors in extremely cold environments.

ADVANCED MATERIALS TECHNOLOGIES
www.advmattechnol.de

Antifreeze Polyvinyl Alcohol Organohydrogel Sensors Containing Polypyrrole Nanowires Self-Assembled onto Graphene Oxide Nanoplatelets with High Electrical Conductivity and Improved Mechanical Properties

Pengcheng Yang, Junwei Bai, Federico Olivieri, Chiara Santillo, Rachele Castaldo, Gennaro Gentile, Junhua Zhang, Marino Lavorgna,* and Giovanna G. Buonocore*

Conductive hydrogels exhibit significant potential for flexible electronics owing to their exceptional flexibility, resistance to deformation, and high conductivity. However, there is a critical need to develop hydrogels that can withstand extremely low temperatures while exhibiting good mechanical properties. In this study, carboxyl-modified polyvinyl alcohol (PVA) as the gel matrix, dimethylsulfoxide and water as a mixed solvent solution, and graphene oxide (GO) assembled polypyrrole (PPy) nanowires are used to prepare a new type of antifreeze conductive organohydrogel (PGOPPy). The PGOPPy organohydrogel demonstrates outstanding antifreeze properties, retaining its flexibility at temperatures as low as −75 °C. It exhibits a fracture strength of 0.80 MPa and an elongation at break of 436% at room temperature. Remarkably, after being stored at room temperature for 15 days, the diameter of the PGOPPy organohydrogel changes only by 4%. Moreover, PGOPPy shows high electrical conductivity, up to 1.07 S m^{-1}, and exhibits variable conductivity in response to mechanical deformation, with a stable response over cyclic deformations, allowing its use as a sensor to monitor body movements. Results demonstrate that the developed material is very promising as an effective sensor technology for use in extremely cold environments. Moreover, this work provides a general method for preparing antifreeze organhydrogels using water and dimethylsulfoxide as mixed solvents.

1. Introduction

Over the past two decades, flexible electronics have gained increasing attention due to their remarkable flexibility and signal conversion capabilities.[1–5] Conductive hydrogels are frequently employed in fabricating wearable devices owing to their flexibility and capacity to conduct electrical signals.[6–8] However, hydrogels used in wearable devices suffer from two critical drawbacks. First, hydrogels primarily composed of water tend to stiffen below 0 °C when employed in wearable devices,[9–11] rendering them impractical. Second, most of the hydrogels realized so far exhibit low mechanical strength.[12,13]

To develop hydrogels able to work in harsh conditions for low temperatures, researchers usually replace water in hydrogels with an organic solvent with a very low freezing point, such as glycerol.[14,15] However, this method is a two-step process, based on a complex water replaced with the selected organic solvent without affecting the structure of the gel.[16,17] Another method

P. Yang, F. Olivieri, R. Castaldo, G. Gentile
Institute of Polymers, Composites, and Biomaterials
National Council of Research of Italy
Via Campi Flegrei, 34, Pozzuoli, NA 80078, Italy
E-mail: gennaro.gentile@cnr.it

P. Yang
Dipartimento Scienza Applicata e Tecnologia (DISAT)
Politecnico di Torino
Corso Duca degli Abruzzi, 24, Torino 10129, Italy

The ORCID identification number(s) for the author(s) of this article can be found under https://doi.org/10.1002/admt.202400970

DOI: 10.1002/admt.202400970

J. Bai
China Bluestar Chengrand Chemical Co. Ltd
Chengdu 610041, China

C. Santillo, M. Lavorgna, G. G. Buonocore
Institute of Polymers, Composites and Biomaterials
National Council of Research of Italy
P.le E. Fermi, 1, Portici, NA 80155, Italy
E-mail: marino.lavorgna@cnr.it

J. Zhang
The State Key Laboratory of Polymer Materials Engineering
Polymer Research Institute of Sichuan University
Chengdu 610065, China

to enhance the frost resistance of hydrogels involves adding salts, such as sodium chloride and calcium chloride, to the hydrogel system.[18–20] Hydrogels produced using this approach well perform at temperatures below 0 °C and exhibit some electrical conductivity. However, challenges arise when they are used at extremely low temperatures.[21]

Polyvinyl alcohol (PVA) dissolved in an aqueous solution gives rise to hydrogels that exhibit fracture strengths of less than 0.3 MPa.[22] This low strength poses a risk of rupture damage when utilized in wearable devices. To address this issue, researchers have developed hydrogels with double-network (DN) structure and added some 2D filler to enhance strength.[23,24] DN hydrogels, composed of two interpenetrating or semi-penetrating polymer networks, exhibit superior mechanical strength or toughness compared to each network alone.[25,26] Graphene oxide (GO) nanosheets are a commonly used material to enhance the strength of hydrogels, and its flake structure, with hydroxyl and carboxyl groups on its surface, is beneficial to its dispersion in hydrogel systems.[27–30] Nonetheless, the conductivity of graphene oxide alone is weak, restricting its utility in wearable applications mainly as a reinforcing agent.[31,32] To improve the electrical conductivity of GO, thermal or chemical methods to reduce GO to reduced graphene oxide (rGO) can be used.[27] Nevertheless, thermal GO reduction is unsuitable for organohydrogels because it induces solvent evaporation, whereas chemical reduction methods require the addition to the gel formulation of a reducing agent that must be removed at the end of the reduction process, with difficulties especially when mixed solvent mixtures are used for the organohydrogel preparation as the removal of the reducing agent can modify the relative amounts of the gel components.

Polypyrrole (PPy) nanowires exhibit both excellent electrical conductivity and good dispersibility in aqueous dispersions. To improve the electrical conductivity of GO, assembling with PPy nanowires, exploiting —OH and —COOH surface GO groups that can interact with the —NH of PPy by hydrogen bonding, is an effective approach.[33–35] Moreover, dimethylsulfoxide (DMSO) and water (H_2O) are very good solvents for PVA, and when DMSO and H_2O are mixed in a molar ratio of 1:3, they are still fluid at −70 °C.[36,37] This behavior inspired the development of PVA organohydrogels with anti-freezing properties utilizing DMSO and H_2O as mixed solvents.[38,39]

Starting from this background, new PVA organohydrogels with enhanced freeze-resistance and electrical conductivity by embedding in the gel properly synthesized GO assembled with PPy nanowires (GOPPy) have been produced in this research. The microscopic morphology, intermolecular forces, and mechanical properties of PVA organohydrogel (P), PVA-GO organohydrogel (PGO), and PVA-GOPPy (PGOPPy) organohydrogel were characterized by field emission scanning electron microscopy (FE-SEM), transmission electron microscope (TEM), Fourier-transform infrared spectrometer (FT-IR), and tensile tests. The obtained PGOPPy organohydrogel exhibits very good performance, including enhanced tensile strength and elongation. Compared to other methods, the proposed approach does not require the addition of any salts or solvent exchange processes, and the gel remains flexible even at −75 °C. Noticeably, this PGOPPy organohydrogel is suitable to be applied as a flexible sensor to monitor human joint deformation in ultra-low temperature environments.

2. Experimental Section

2.1. Materials

Graphene oxide (GO, 2% dry content, Aspect ratio = 10, Guoheng Co., Ltd), ammonium persulfate (APS, $(NH_4)_2S_2O_8$, 98%, Huaxia reagent Co., Ltd), dimethylsulfoxide (DMSO, C_2H_6SO, 98%, Huaxia reagent Co., Ltd) and pyrrole (Py, C_4H_5N, 98%, Huaxia reagent Co., Ltd), hexadecyl trimethyl ammonium bromide (CTAB, $C_{19}H_{42}BrN$, 98%, Huaxia reagent Co., Ltd), carboxyl modified poly(vinyl alcohol) (coded as PVA, C-PVA-1899, degree of polymerization 1800, alcoholysis degree 99%, carboxyl content 5%, Sinopec Sichuan vinylon works).

2.2. Preparation of PVA Organohydrogels (P)

The typical P organohydrogel was prepared by freeze-thaw methods. First, 15 g of PVA were dissolved in a mixed solution of DMSO (50.23 g, 0.64 mol) and H_2O (34.77 g, 1.93 mol) at 90 °C. Then, the homogeneous solution was cooled down to room temperature and transferred into a Petri dish. The solution was placed in a refrigerator at −20 °C for 12 h to promote gel formation, then the system was brought to room temperature and left for 4 h. The cooling-room temperature cycle was repeated three times to obtain P organohydrogel.

2.3. Preparation of PVA-GO Organohydrogels (PGO_x)

The typical PGO_x organohydrogel was prepared by physical mixing and freeze-thaw method. First, 15 g of PVA was dissolved in a mixed solution of DMSO (50.23 g, 0.64 mol) and H_2O (34.77 g, 1.93 mol) at 90 °C. Then, different amounts of GO (0.15, 0.23, 0.30, 0.38, and 0.45 g) were dispersed in the previous PVA solution. Subsequently, the mixtures were mechanically stirred vigorously for 30 min and left to stand at room temperature for 2 h. Finally, to obtain the PGO_x organohydrogel, the samples were treated by freeze-thawing three times as detailed for the P organohydrogels, where x (= 1, 1.5, 2, 2.5, and 3, respectively) is the per hundred resin (phr) GO content based on the dry PVA weight.

2.4. Preparation of PVA Modified with Polypyrrole Nanowires Assembled on GO Organohydrogels ($P(GO_zPPy_w)_x$)

$P(GO_zPPy_w)_x$ organohydrogels were prepared by adding different pyrrole-assembled GO to the PVA solution. With this objective, GO samples assembled with different amounts of PPy were prepared as follows. First, 25 mL of GO dispersion (20 mg mL^{-1}) was diluted to 200 mL (dry GO content: 0.5 g). Subsequently, CTAB (0.46, 0.91, 1.37, 1.82, 2.28, 2.73, 3.19, and 3.64 g) and Py (0.13, 0.27, 0.40, 0.53, 0.66, 0.80, 0.93, and 1.06 g) were added. The mixture was fast mechanically stirred for 30 min, then it was put into an ice bath at 0 °C. APS (0.46, 0.91, 1.37, 1.82, 2.28, 2.74, 3.19, and 3.65 g) in 40 mL HCl solution (1 mol L^{-1}) were added to the above dispersion, stirred for 3 h, and then left to stand overnight at 0 °C. After that, the mixture was rinsed with deionized water to remove

Table 1. Codes and compositions of the prepared samples.

Code	PVA solution [g]	GO [g]	GO_zPPy_w [g]
P	100	–	–
PGO_x organohydrogels			
$PGO_{1.0}$	100	0.15	–
$PGO_{1.5}$	100	0.23	–
$PGO_{2.0}$	100	0.30	–
$PGO_{2.5}$	100	0.38	–
$PGO_{3.0}$	100	0.45	–
$P(GO_zPPy_w)_x$ organohydrogels			
$P(GO_{0.80}PPy_{0.20})_{2.5}$	100	–	0.375
$P(GO_{0.66}PPy_{0.34})_{3.0}$	100	–	0.450
$P(GO_{0.29}PPy_{0.71})_{3.5}$	100	–	0.525
$P(GO_{0.50}PPy_{0.50})_{4.0}$	100	–	0.600
$P(GO_{0.44}PPy_{0.56})_{4.5}$	100	–	0.675
$P(GO_{0.40}PPy_{0.60})_{5.0}$	100	–	0.750
$P(GO_{0.36}PPy_{0.64})_{5.5}$	100	–	0.825
$P(GO_{0.33}PPy_{0.67})_{6.0}$	100	–	0.900

CTAB. The obtained product was subsequently placed in an oven and dried at 60 °C for 24 h.[40,41] The prepared pyrrole-assembled GO materials were coded as GO_zPPy_w, where z and w are the mass fractions of GO and PPy, respectively. The following systems were prepared: $GO_{0.80}PPy_{0.20}$, $GO_{0.66}PPy_{0.34}$, $GO_{0.29}PPy_{0.71}$, $GO_{0.50}PPy_{0.50}$, $GO_{0.44}PPy_{0.56}$, $GO_{0.40}PPy_{0.60}$, $GO_{0.36}PPy_{0.64}$, and $GO_{0.33}PPy_{0.67}$.

The GO_zPPy_w materials synthesized as above described were then used for the preparation of $P(GO_zPPy_w)_x$ organohydrogel, as detailed as follows. The prepared black solids GO_zPPy_w were added to 100 g of PVA solution (dry content 15 wt.%). Then, by applying the above-described 3-cycle freeze-thaw method, the $P(GO_zPPy_w)_x$ organohydrogels, where x is the content of GO_zPPy_w (phr) related to the dry PVA content in the organohydrogels. The codes and compositions of the prepared samples are summarized in **Table 1**.

2.5. Characterization

2.5.1. Characterization of GO Assembled with PPy Nanowires

The morphology of the functional $GO_{0.50}PPy_{0.50}$ filler was investigated by TEM using a Tecnai G12 Spirit Twin TEM equipped with a 4k FEI CCD camera. FT-IR analysis of $GO_{0.50}PPy_{0.50}$ was performed using a Perkin Elmer One FT-IR spectrometer. By comparison, GO and PPy were also analyzed through FT-IR in the 4000–600 cm^{-1} region. The electrical conductivity of $GO_{0.50}PPy_{0.50}$ was analyzed by using a Keithley electrometer equipped with an SR-4 probe stand and an SR H40 T four-point probe head.

2.5.2. Characterization of Organohydrogels

The morphology of P, PGO_x and $P(GO_zPPy_w)_x$ organohydrogels was investigated by FE-SEM (Nova NanoSEM450). TEM (JEOL-JEM 2100) was employed to observe the microstructure during the formation of antifreeze and moisturizing conductive organohydrogels. FT-IR spectra of the gels were acquired using an FT-IR spectrometer Nicolet-560 in the 4000–400 cm^{-1} region. Long strip-like organohydrogels with a width of 10 mm and a length of 50 mm were prepared. Tensile test was carried out at room temperature using an electronic universal testing machine (CMT4202/ZWICK/Z020). The rate of the extension was fixed at 20 mm min^{-1} for the tensile test. The four-probe tester RT-3000/RG-2000(3000) was used to measure the conductivity of the $P(GO_zPPy_w)_x$ organohydrogel. The organohydrogel was cut into strips measuring 4 cm in length and 1 cm in width, with copper wires attached on both ends. The organohydrogel was then wrapped in cling film and secured to the finger and elbow for real bending motion experiments, performed trying to maintain the same speed and final angle during the bending of fingers and elbows. The change in resistance or current signal of the organohydrogel during stretching or compression was measured in real-time by a Keithley 2601B (USA) single-channel source meter. The change of $\Delta R/R_0$ was employed to record the change of the sensor monitoring signal.[42] The ΔR value of samples was defined as follows: $\Delta R = R\text{-}R_0$, where R and R_0 present the resistance value of organohydrogel with and without deformation, respectively. The frost resistance of $P(GO_zPPy_w)_x$ organohydrogel was tested by placing it in a dry ice-ethanol mixed bath at −75 °C for 2 h. After taking it out, visual inspection and tackle bending motion were performed to evaluate its appearance and confirm the persistence of suitable flexibility.

2.5.3. Combined Energy Calculations

Molecular dynamics simulations were performed to calculate the interactions between PVA molecular chains and GO nanosheets in PGO_x organohydrogel, and PVA molecular chains, GO nanosheets, and PPy molecular chains in $P(GO_zPPy_w)_x$ organohydrogel. The molecular dynamic simulation was performed under a universal force field in Material Studio 2018. First, models of the PPy molecule and the GO nanosheets were constructed and geometrically optimized using the Forcite module. The GO (0 0 −1) layer was cleaved and then modeled using 10 × 7 supercells. Then, in performing the adsorption locator simulation, three PPy molecules with five degrees of polymerization were randomly distributed on the surface of the GO layer with a maximum adsorption distance of 15 Å. Next, the amorphous structure of PVA was constructed by a predigested method. To build the model of PVA, five molecular chains of PVA with forty degrees of polymerization, five molecules of DMSO and ten molecules of H_2O were built, and then geometrical optimization was performed. After each constituent was modeled, the overall system was built with a minimum initial energy. Furthermore, the isothermal-isochoric molecular dynamic simulations of GO-PVA composite and PPy-GO-PVA composite models were carried out at 298 K. During the simulation, the position of the GO (0 0 −1) layer was fixed, but the polymer chains and PPy were allowed to adjust conformation. Finally, the binding energy can be calculated based on the following equation: $E_{bind} = E_{(A)} + E_{(B)} - E_{(AB)}$, where $E_{(A)}$ and $E_{(B)}$ are the energies of subsystems A and B, and $E_{(AB)}$ is the energy of the compound system.

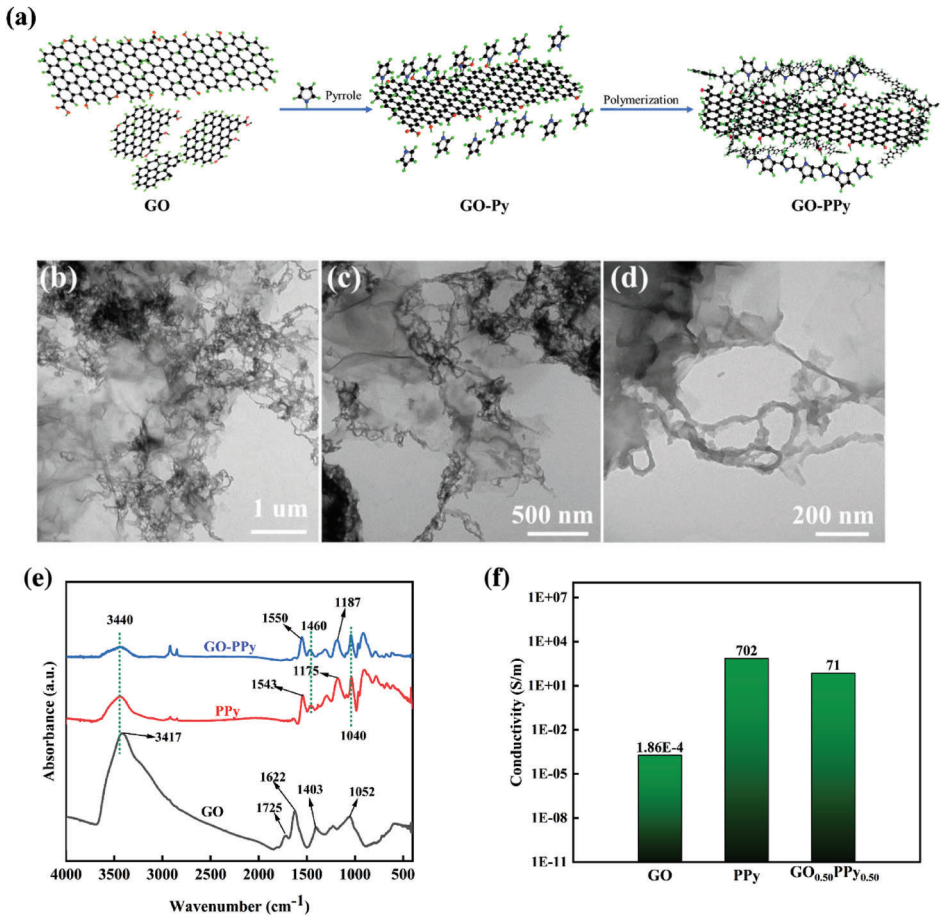

Figure 1. a) Schematic illustration of the assembling mechanism of PPy onto GO in the GO_zPPy_w samples; b-d) TEM images of $GO_{0.50}PPy_{0.50}$; e) FT-IR spectra of GO, PPy and $GO_{0.50}PPy_{0.50}$; f) electrical conductivity of GO, PPy and $GO_{0.50}PPy_{0.50}$.

3. Results and Discussion

3.1. Characterization of GO_zPPy_w Hybrid Filler

Graphene oxide assembled polypyrrole nanowire composite material (GO_zPPy_w) was synthesized using an in situ chemical polymerization method. In this process, the solution of pyrrole monomer and graphene oxide was vigorously stirred in the presence of CTAB. The carboxyl, hydroxyl, and epoxy groups in GO are situated on the surface and edges of the nanosheets of GO. As depicted in **Figure** 1a, these groups promote the assembling of the pyrrole monomer as well as polypyrrole nanowires, after triggering polymerization by APS addition, onto the GO surface through hydrogen bonding and π–π stacking interactions.[43]

As shown in Figure 1b–d, TEM analysis confirmed the successful assembling of PPy onto the surface of GO in the $GO_{0.50}PPy_{0.50}$ sample, with the formation of PPy nanowires that effectively link together different GO sheets. Figure 1e shows the FT-IR spectrum of the GO, PPy, and $GO_{0.50}PPy_{0.50}$. The FT-IR spectrum of GO exhibits a strong peak at 3417 cm^{-1}, with additional peaks of lower intensity observed at 1725, 1622, 1403, and 1052 cm^{-1}. These peaks correspond to the –OH group, stretching of the carboxylic acid group, remaining sp^2 hybridized C groups after oxidation tertiary C—OH group, and C—O stretching vibrations of alkoxy groups, respectively.[44] The peaks of $GO_{0.50}PPy_{0.50}$ at 1187, 1460, and 1550 cm^{-1} are related to the tensile vibration of C—H, C=C, and CN in PPy nanowires, respectively.[45] Due to the stronger electrophilic induction effect of the oxygen atoms on the GO layers compared to the mentioned π–π conjugate effect, the vibration peak of the pyrrole ring (1543 cm^{-1}) shifts to a higher wavenumber (1550 cm^{-1}).[33] Compared the spectrum of $GO_{0.50}PPy_{0.50}$ with those of GO and PPy reveals for $GO_{0.50}PPy_{0.50}$ a shift in the peak positions of C—N, C—H, and H—N of GO-PPy nanowires, suggesting the effective assembling of PPy nanowires onto GO. These findings confirm the interaction between pyrrole and oxygen atoms of GO, indicating that polymerized pyrrole is effectively assembled on the surface of GO layers.

The four-probe conductivity tests (Figure 1f) indicate that GO is essentially non-conductive (1.86×10^{-4} S m^{-1}), while the conductivity of PPy is 702 S m^{-1}. By assembling the same weight (Py, 2 phr) of PPy nanowires onto the GO sheets ($GO_{0.50}PPy_{0.50}$), the measured conductivity is 71 S m^{-1}. All the results confirm that pyrrole was effectively polymerized into nanowires on the surface of GO, with polypyrrole nanowires serving to interconnect different GO nanosheets, significantly enhancing the GO electrical conductivity by about five orders of magnitude. This makes it possible to be used to develop conductive organohydrogels.

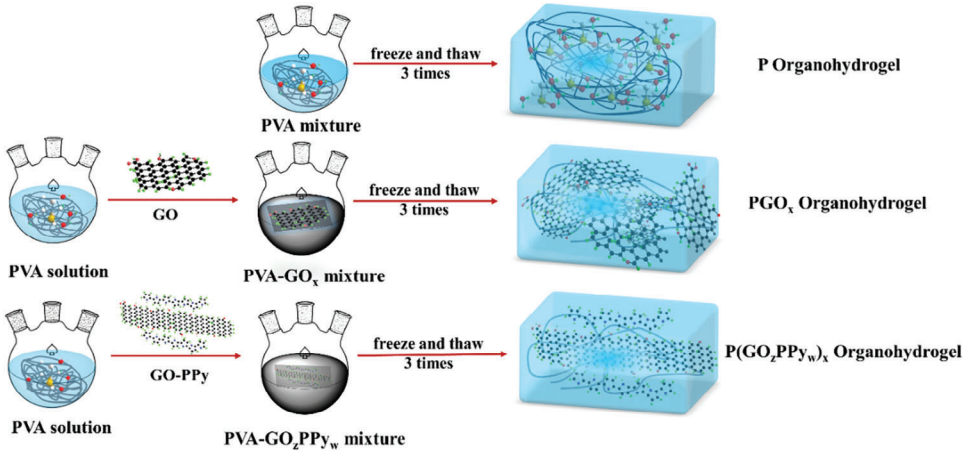

Figure 2. The formation mechanism of P organohydrogel, PGO$_x$ organohydrogel, P(GO$_z$PPy$_w$)$_x$ organohydrogel.

3.2. Formation Mechanism of P, PGO$_x$, and P(GO$_z$PPy$_w$)$_x$ Organohydrogel

P(GO$_z$PPy$_w$)$_x$ organohydrogels were prepared by incorporating GO$_z$PPy$_w$ composite materials into P organohydrogel. The preparation schematics of P, PGO$_x$ and P(GO$_z$PPy$_w$)$_x$ organohydrogels are illustrated in **Figure 2**.

3.3. The Properties of P, PGO$_x$, and P(GO$_z$PPy$_w$)$_x$ Organohydrogels

To investigate the effect of GO addition on the mechanical properties of PGO$_x$ organohydrogel, we performed tensile tests at room temperature on PGO$_x$ organohydrogels with different contents of GO. As shown in **Table 2** and **Figure 3a**, Young's modulus, the tensile strength and elongation at break of the P organohydrogel are 0.11 GPa, 0.30 MPa, and 302%, respectively. By GO addition, Young's modulus and tensile strength of the organohydrogels increase until the GO content reaches 1.5 phr and then progressively decreases as the GO content further increases. This is because when the GO content in the PGO organohydrogel is ≤ 1.5 phr, GO is stable and uniformly dispersed in the PVA mixed solution of H_2O and DMSO. There is a strong interaction between GO nanosheets and PVA molecular chains, which increases the resistance to deformation and, consequently, the Young's modulus as the GO content increases. However, when the GO content exceeds 1.5 phr, the GO concentration becomes too high to remain stably and uniformly dispersed in the PVA mixture, leading to aggregation. This reduces the PGO organohydrogel's ability to resist deformation, and thus the Young's modulus decreases. On the other hand, while almost all PGO$_x$ organohydrogels show elongation at break comparable or lower to the P sample, the sample containing 2 phr of GO shows the highest elongation at break (448%) in comparison to the pristine PVA gel. This is attributed to the hydrogen bond interactions between hydroxyl, carboxyl, and epoxy groups on GO nanosheets and hydroxyl groups on the PVA molecular chains[43] as well as to the stacking of GO nanoplatelets. The sample PGO$_2$ shows Young's modulus of 0.15 GPa and tensile strength of 0.64 MPa, which are slightly lower than the maximum values exhibited by PGO$_{1.5}$, therefore representing the best compromise in terms of mechanical properties. For this reason, the P(GO$_z$PPy$_w$)$_x$ organohydrogels were prepared using different GO$_z$PPy$_w$ hybrid fillers after fixing the GO content at 2 phr (according to the formulations reported in Table 1).

As shown in Figure 3b, tensile tests were conducted on the P(GO$_{0.50}$PPy$_{0.50}$)$_4$ organohydrogel. When polypyrrole assembled onto GO was introduced at 2 phr, the tensile strength of P(GO$_{0.50}$PPy$_{0.50}$)$_4$ organohydrogel reached 0.80 MPa, and the elongation at break was 436%, similar to that shown by PGO$_2$. This is because the polypyrrole nanowires effectively self-assemble onto GO nanoplatelets and contribute to building up a network by maximizing interfacial interactions between hybrid fillers and the PVA macromolecules with consequent increment

Table 2. Tensile properties of PGO$_x$ and P(GO$_{0.50}$PPy$_{0.50}$)$_4$ organohydrogel.

Sample	Young's Modulus [GPa]	Elongation at break [%]	Fracture strength [MPa]	Toughness [MJ m^{-3}]
P	0.11 ± 0.01	302 ± 11	0.30 ± 0.03	0.52
PGO$_1$	0.14 ± 0.02	253 ± 15	0.32 ± 0.02	0.50
PGO$_{1.5}$	0.23 ± 0.02	299 ± 11	0.68 ± 0.02	1.17
PGO$_2$	0.15 ± 0.01	448 ± 8	0.64 ± 0.04	1.65
PGO$_{2.5}$	0.10 ± 0.01	298 ± 6	0.28 ± 0.02	0.43
PGO$_3$	0.08 ± 0.01	147 ± 5	0.12 ± 0.01	0.07
PGO$_{(0.50}$PPy$_{0.50)4}$	0.18 ± 0.02	436 ± 10	0.80 ± 0.04	1.87

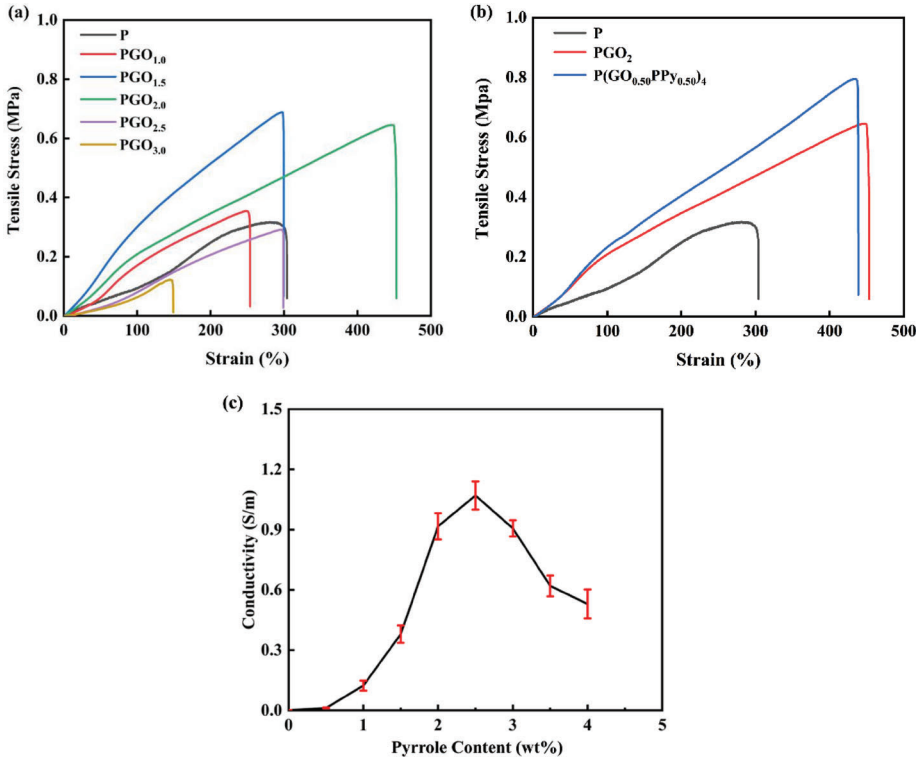

Figure 3. a) Stress–strain curve of PGO_x organohydrogel with different content of GO; b) stress–strain curve of P, PGO_2, and $P(GO_{0.50}PPy_{0.50})_4$; c) electrical conductivity of $P(GO_{0.50}PPy_w)_x$ organohydrogels.

in both elongations at break and tensile strength in comparison to plain PVA hydrogel. Toughness is the energy absorbed by a material before it fractures, representing the material ductility and impact resistance. When the GO content is ≤ 2 phr, the toughness increases with the increase in GO content. When the GO content reaches 2 phr, the fracture toughness of the PGO organohydrogel reaches a maximum of 1.65 MJ m^{-3}. This is because the addition of GO connects the PVA molecular chains, increasing toughness. However, when the GO content exceeds this level, the toughness significantly decreases due to GO aggregation, resulting in a non-uniform system and creating stress weak points that lead to reduced toughness. The addition of PPy further increases the toughness because the PPy nanowires connect different GO nanosheets and PVA molecular chains, thereby increasing the toughness to 1.87 MJ m^{-3}. To further substantiate this evidence, molecular dynamics calculations were carried out (for details about the dynamics calculations see Supporting Information). The results confirm that the binding energy of the PGO organohydrogel system is 297 kJ mol^{-1} whereas that for PGOPPy organohydrogel system is 674 kJ mol^{-1}. This difference is attributed to the tighter binding between PVA, GO, and PPy molecules due to the introduction of PPy. Therefore, the presence of PPy assembled onto GO nanoplatelets improves the mechanical properties of organohydrogels, consistently with the results of tensile tests.

Moreover, introducing polypyrrole nanowires into PGOx organohydrogel results in the formation of $P(GO_zPPy_w)_x$ conductive organohydrogel. As shown in Figure 3c, conductivity tests reveal that at 2.5 phr polypyrrole content the conductivity of $P(GO_{0.44}PPy_{0.56})_{4.5}$ is 1.07 S m^{-1}. However, at this concentration, the elasticity of the organohydrogel decreases. The electrical conductivity of $P(GO_{0.5}PPy_{0.5})_4$ is 0.91 S m^{-1}; therefore, the difference between $P(GO_zPPy_w)_x$ organohydrogels with $GO_{0.50}PPy_{0.50}$ (2 phr polypyrrole content) and $GO_{0.44}PPy_{0.56}$ (2.5 phr polypyrrole content) is negligible. For further tests, the PGOPPy organohydrogel containing 2 phr of polypyrrole assembled onto GO ($P(GO_{0.50}PPy_{0.50})_4$) was selected.

Optical images of $PGO_{0.50}PPy_{0.50}$ and P organohydrogels are reported in **Figure 4a**.

As shown, the color of the organohydrogel changes from colorless P organohydrogel to the black of $P(GO_{0.50}PPy_{0.50})_4$ organohydrogel due to the presence of GO-assembled polypyrrole nanowires. As shown in Figure 4b, after being stored at room temperature for 15 days, minimal changes are observed in the diameter of the $P(GO_{0.50}PPy_{0.50})_4$ organohydrogel. This suggests that the organohydrogel formulated with carboxyl-modified PVA as its base material exhibits excellent moisture retention properties[22,46] and the filler is able to counterbalance the shrinkage due to the water release. This has been confirmed in previous studies.[22] The $P(GO_{0.50}PPy_{0.50})_4$ organohydrogel can still bend, showing good flexibility, when placed in a dry ice ethanol bath at −75 °C (Figure 4c). This is because strong hydrogen bonds can form between water and DMSO molecules. At low temperatures, the likelihood of significant rearrangement within the hydrogen bond network diminishes. Consequently, a relatively rigid and structurally diverse network gradually forms, hindering the development of a crystalline-like order.[47,48] Remarkably all organohydrogels, namely P, PGO_x, and

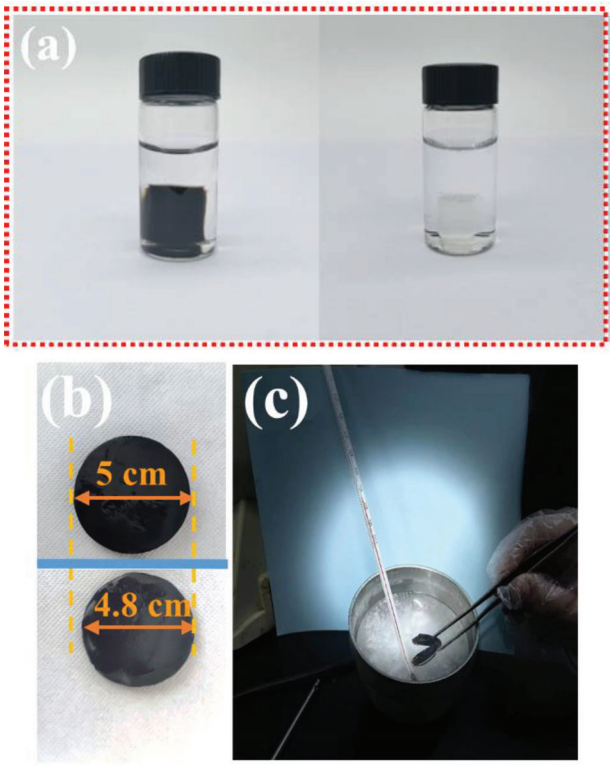

Figure 4. a) Optical images of the P and the $P(GO_{0.50}PPy_{0.50})_4$ organohydrogels; b) image of the $P(GO_{0.50}PPy_{0.50})_4$ organohydrogels after 15 days at room temperature; c) image of the $P(GO_{0.50}PPy_{0.50})_4$ organohydrogel at −75 °C.

$P(GO_zPPy_w)_x$ organohydrogels, exhibit similar anti-freezing properties at −75 °C.

The PGO_2 and the $P(GO_{0.50}PPy_{0.50})_4$ organohydrogels after solvent removal were analyzed by TEM and SEM tests to observe their microstructure and morphology. TEM and SEM analysis of PGO_2 (**Figure** 5a,b) revealed a good dispersion of the GO phase in the PVA organohydrogel. Similarly, also in the $P(GO_{0.50}PPy_{0.50})_4$ organohydrogel (Figure 5c,d), it is well evident that $GO_{0.50}PPy_{0.50}$ is homogeneously distributed in the PVA. This effective dispersion of GO and GO-assembled PPy nanowires in the PVA phase is attributed to good interactions of the carboxyl and hydroxyl groups of —COOH functionalized PVA with the amino group of polypyrrole and the —OH and —COOH groups of GO.

The structure and intermolecular interactions of P, PGO_2, and $P(GO_{0.50}PPy_{0.50})_4$ organohydrogels were examined by FT-IR. Spectra are shown in Figure 5e. As for P organohydrogel, the broad adsorption band at 3280 cm^{-1} corresponds to the O—H stretching vibration, and peaks at 2939 and 2902 cm^{-1} represent the asymmetric and symmetric stretching vibration of the $—CH_2$ group.[49] Additionally, the peak at 1716 cm^{-1} corresponds to the C=O stretching vibration of the —COOH group,[50] while the peak at 1090 cm^{-1} represents the stretching vibration of the C—O bond[51] confirming the presence of PVA modified with COOH groups. When GO was added to form the PGO_2 organohydrogel, a reduction in the peaks ≈1716 cm^{-1} was observed, indicating an interaction between the —COOH groups in PVA and the —OH groups of GO, resulting in peak shifts. The spectrum also displays a peak at 1620 cm^{-1} can be attributed to the stretching vibration of C=C confirming the presence of GO into the organohydrogel.[52] Additionally, the FT-IR spectrum of $P(GO_{0.50}PPy_{0.50})_4$ reveals two peaks at 1646 and 1568 cm^{-1}, likely due to the π–π conjugate effect between the C=C bonds of pyrrole and the lone pair electrons of oxygen atoms in GO layers.[51] The results confirm that $GO_{0.50}PPy_{0.50}$ hybrid filler exhibited excellent dispersion within the mixture of carboxyl-modified PVA, DMSO, and H_2O.

3.4. Application as a Sensor

The conductive hydrogel can be applied to wearable devices, reflecting mechanical changes through current changes.[53–55] The sensor made from $P(GO_{0.50}PPy_{0.50})_4$ organohydrogel can also be used for the detection of large deformation. Fixing the organohydrogel on the finger or elbow, the bending movement of the finger and elbow can be detected by the current value.

The resistance value of the organohydrogel when the finger or elbow joint is not bent is denoted as R0 (see **Figures** 6a–c). When the finger joint is bent at 45°, 60°, and 90°, the PPy conductive network within the $P(GO_{0.50}PPy_{0.50})_4$ organohydrogel sensor is stretched, causing physical separation of the conductive particles, thereby reducing the resistance value and resulting in the maximum $\Delta R/R_0$. By repeating the bending process of the finger or elbow, the $P(GO_{0.50}PPy_{0.50})_4$ organohydrogel sensor consistently records the joint deformation. Additionally, it can also be used to record specific bending angles of finger movements, providing more precise sensing of finger bends. Figure 6c shows that the $\Delta R/R_0$ change value of the PGOPPy sensor is 1.7 when the finger is bent at 90°, while similar sensors reported in literature have a value of 0.6,[14,56] indicating that our sensor has a better response to deformations. This shows that the $P(GO_{0.50}PPy_{0.50})_4$ organohydrogel preparation is suitable for application as a flexible sensor for a stable and precise recording of human body movements.

4. Conclusion

By exploiting the interaction between PPy nanowires and GO sheets with PVA molecular chains, coupled with the low freezing point properties of a mixed solution of DMSO and water, a novel PGOPPy anti-freeze organohydrogel has been successfully synthesized. The inclusion of PPy nanowires significantly improves the mechanical performance of the $P(GO_zPPY_w)_x$ organohydrogel. Incorporating 2 phr GO and 2 phr PPy relative to the weight of PVA, the $P(GO_{0.50}PPy_{0.50})_4$ organohydrogel exhibits a fracture strength of 0.80 MPa and an elongation at a break of 436%. The polymerization of PPy onto GO confer electrical conductivity to the hybrid structure and the $P(GO_zPPY_w)_x$ organohydrogels. The $P(GO_{0.50}PPy_{0.50})_4$ organohydrogel maintains its flexibility even at −75 °C, and its dimensions are unchanged after 15 days of storage at room temperature. When applied to sensors for recording human body movements, this organohydrogel demonstrates the stability of recorded deformation, enabling the

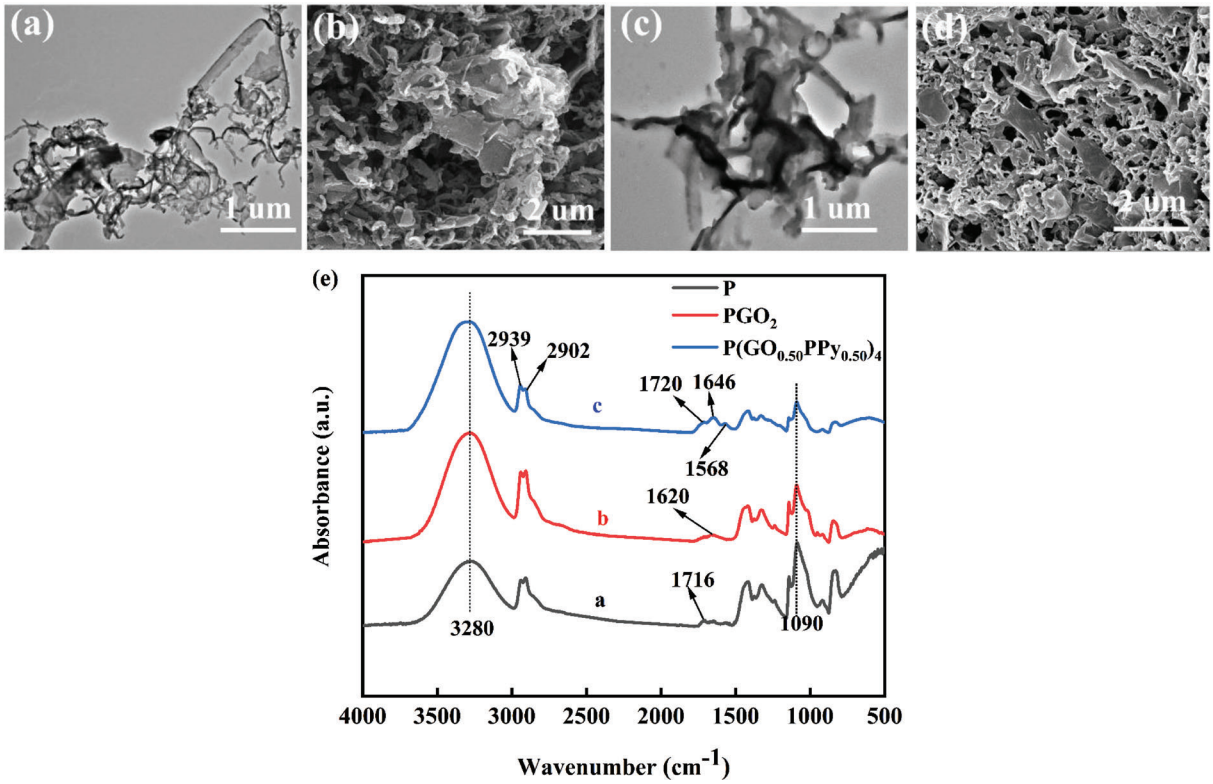

Figure 5. a,b) TEM and SEM images of the PGO_2 organohydrogel; c,d) TEM and SEM images of the $P(GO_{0.50}PPy_{0.50})_4$ organohydrogel; e) FT-IR spectra of P, PGO_2, and $P(GO_{0.50}PPy_{0.50})_4$ organohydrogels.

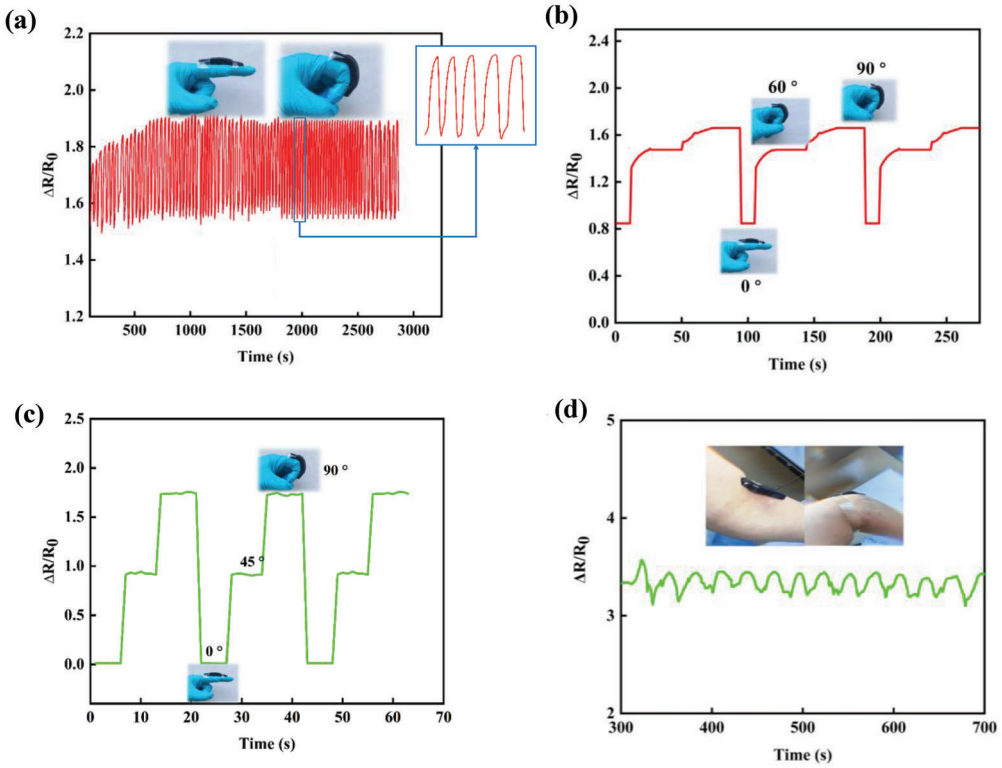

Figure 6. Electrical response of the $P(GO_{0.50}PPy_{0.50})_4$ organohydrogel applied to cyclic joint movements: a) finger flexion; b) elbow flexion.

accurate tracking of finger and elbow joint flexions. Therefore, this research holds promise for application in the field of low-temperature flexible sensors, providing innovative avenues for the fabrication of sensors for low-temperature flexible wearable devices.

Supporting Information

Supporting Information is available from the Wiley Online Library or from the author.

Acknowledgements

This work was supported by Next Generation EU within the Italian National Recovery and Resilience Plan (NRRP), under the project for the realization of an "Infrastructure for Energy Transition and Circular Economy @ EuroNanoLab" (iENTRANCE@ENL), funded by MUR (call Research Infrastructures D. D. n. 3264-IR/2021, CUP: B33C22000710006). Thanks are due to the Extended Partnership PE00000004 "Made in Italy Circolare e Sostenibile" (MICS) project, funded by the European Union-Next Generation EU, for financial support, CUP: B53C22004100001.

Open access publishing facilitated by Consiglio Nazionale delle Ricerche, as part of the Wiley - CRUI-CARE agreement.

Conflict of Interest

The authors declare no conflict of interest.

Data Availability Statement

The data that support the findings of this study are available from the corresponding author upon reasonable request.

Keywords

GO, organohydrogel, polyvinyl alcohol, PPy nanowires, sensor

Received: June 18, 2024
Revised: July 25, 2024
Published online:

[1] H. Ling, S. Liu, Z. Zheng, F. Yan, *Small Methods* **2018**, *2*, 1800070.
[2] T. He, Q. Shi, H. Wang, F. Wen, T. Chen, J. Ouyang, C. Lee, *Nano Energy* **2019**, *57*, 338.
[3] X. Wang, Z. Bai, M. Zheng, O. Yue, M. Hou, B. Cui, R. Su, C. Wei, X. Liu, *J. Sci.: Adv. Mater. Devices* **2022**, *7*, 100451.
[4] J. Li, Q. Ding, H. Wang, Z. Wu, X. Gui, C. Li, N. Hu, K. Tao, J. Wu, *Nano-Micro Lett.* **2023**, *15*, 105.
[5] K. Zhai, H. Wang, Q. Ding, Z. Wu, M. Ding, K. Tao, B. R. Yang, X. Xie, C. Li, J. Wu, *Adv. Sci.* **2023**, *10*, 2205632.
[6] C. Cui, Q. Fu, L. Meng, S. Hao, R. Dai, J. Yang, *ACS Appl. Bio Mater.* **2020**, *4*, 85.
[7] H. Wang, Q. Ding, Y. Luo, Z. Wu, J. Yu, H. Chen, Y. Zhou, H. Zhang, K. Tao, X. Chen, *Adv. Mater.* **2024**, *36*, 2309868.
[8] L. Luo, Z. Wu, Q. Ding, H. Wang, Y. Luo, J. Yu, H. Guo, K. Tao, S. Zhang, F. Huo, *ACS Nano* **2024**, *18*, 15754.
[9] G. Chen, J. Huang, J. Gu, S. Peng, X. Xiang, K. Chen, X. Yang, L. Guan, X. Jiang, L. Hou, *J. Mater. Chem. A* **2020**, *8*, 6776.
[10] Y. Li, C. Hu, J. Lan, B. Yan, Y. Zhang, L. Shi, R. Ran, *Polymer* **2020**, *186*, 122027.
[11] X. P. Morelle, W. R. Illeperuma, K. Tian, R. Bai, Z. Suo, J. J. Vlassak, *Adv. Mater.* **2018**, *30*, 1801541.
[12] J. Wu, S. Han, T. Yang, Z. Li, Z. Wu, X. Gui, K. Tao, J. Miao, L. K. Norford, C. Liu, *ACS Appl. Mater. Interfaces* **2018**, *10*, 19097.
[13] Q. Tang, X. Sun, Q. Li, J. Wu, J. Lin, *Colloids Surf. A* **2009**, *346*, 91.
[14] H. Zhang, X. Wu, Z. Qin, X. Sun, H. Zhang, Q. Yu, M. Yao, S. He, X. Dong, F. Yao, *Cellulose* **2020**, *27*, 9975.
[15] X. Dai, Y. Long, B. Jiang, W. Guo, W. Sha, J. Wang, Z. Cong, J. Chen, B. Wang, W. Hu, *Nano Res.* **2022**, *15*, 5461.
[16] H. Zheng, Q. Huang, M. Lu, J. Fu, Z. Liang, T. Zhang, D. Wang, C. Li, *Polymers* **2022**, *14*, 3721.
[17] N. Lu, R. Na, L. Li, C. Zhang, Z. Chen, S. Zhang, J. Luan, G. Wang, *ACS Appl. Energy Mater.* **2020**, *3*, 1944.
[18] M. Zhu, G. Li, X. Zhang, S. Gan, J. Zhai, X. Song, *Mater. Res. Express* **2019**, *6*, 1150c9.
[19] C. Zhang, J. Wang, S. Li, X. Zou, H. Yin, Y. Huang, F. Dong, P. Li, Y. Song, *Eur. Polym. J.* **2023**, *186*, 111827.
[20] X. Sui, H. Guo, C. Cai, Q. Li, C. Wen, X. Zhang, X. Wang, J. Yang, L. Zhang, *Chem. Eng. J.* **2021**, *419*, 129478.
[21] Y. Jian, S. Handschuh-Wang, J. Zhang, W. Lu, X. Zhou, T. Chen, *Mater. Horiz.* **2021**, *8*, 351.
[22] P. Yang, Y. Zhao, J. Zhang, *React. Funct. Polym.* **2022**, *170*, 105089.
[23] Y. Mori, H. Tokura, M. Yoshikawa, *J. Mater. Sci.* **1997**, *32*, 491.
[24] K. Tao, J. Yu, J. Zhang, A. Bao, H. Hu, T. Ye, Q. Ding, Y. Wang, H. Lin, J. Wu, *ACS Nano* **2023**, *17*, 16160.
[25] X. Huang, J. Li, J. Luo, Q. Gao, A. Mao, J. Li, *Mater. Today Commun.* **2021**, *29*, 102757.
[26] K. Tao, Z. Chen, J. Yu, H. Zeng, J. Wu, Z. Wu, Q. Jia, P. Li, Y. Fu, H. Chang, *Adv. Sci.* **2022**, *9*, 2104168.
[27] G. Oxide, in *Reduction Recipes, Spectroscopy, and Applications*, (Ed.: W. Gao), Springer International Publishing, USA **2015**.
[28] A. Chouhan, H. P. Mungse, O. P. Khatri, *Adv. Colloid Interface Sci.* **2020**, *283*, 102215.
[29] A. M. Dimiev, S. Eigler, in *Graphene Oxide: Fundamentals and Applications*, John Wiley & Sons, USA **2016**.
[30] Y. Huang, M. Zhang, W. Ruan, *J. Mater. Chem. A* **2014**, *2*, 10508.
[31] K.-x. Sheng, Y.-x. Xu, L. Chun, G.-q. Shi, *New Carbon Materials* **2011**, *26*, 9.
[32] Z. Wu, X. Yang, J. Wu, *ACS Appl. Mater. Interfaces* **2021**, *13*, 2128.
[33] R. Bissessur, P. K. Liu, S. F. Scully, *Synth. Met.* **2006**, *156*, 1023.
[34] Z. Gu, L. Zhang, C. Li, *J. Macromol. Sci., Part B* **2009**, *48*, 1093.
[35] A. L. Pang, A. Arsad, M. Ahmadipour, *Polym. Adv. Technol.* **2021**, *32*, 1428.
[36] R. N. Havemeyer, *J. Pharm. Sci.* **1966**, *55*, 851.
[37] D. Rasmussen, A. MacKenzie, *Nature* **1968**, *220*, 1315.
[38] K. Yamaura, M. Itoh, T. Tanigami, S. Matsuzawa, *J. Appl. Polym. Sci.* **1989**, *37*, 2709.
[39] K. Yamaura, K. I. Karasawa, T. Tanigami, S. Matsuzawa, *J. Appl. Polym. Sci.* **1994**, *51*, 2041.
[40] A. Wu, H. Kolla, S. K. Manohar, *Macromolecules* **2005**, *38*, 7873.
[41] X. Zhang, J. Zhang, W. Song, Z. Liu, *J. Phys. Chem. B* **2006**, *110*, 1158.
[42] S. Xia, Q. Zhang, S. Song, L. Duan, G. Gao, *Chem. Mater.* **2019**, *31*, 9522.
[43] S. Konwer, R. Boruah, S. K. Dolui, *J. Electron. Mater.* **2011**, *40*, 2248.
[44] F. T. Johra, W.-G. Jung, *Appl. Surf. Sci.* **2015**, *357*, 1911.
[45] A. Yussuf, M. Al-Saleh, S. Al-Enezi, G. Abraham, *Intl. J. Polym. Sci.* **2018**, *2018*, 4191747.
[46] Z. Lian, L. Ye, *J. Polym. Res.* **2015**, *22*, 72.
[47] B. Kirchner, M. Reiher, *J. Am. Chem. Soc.* **2002**, *124*, 6206.
[48] K. I. Oh, K. Rajesh, J. F. Stanton, C. R. Baiz, *Angew. Chem.* **2017**, *129*, 11533.

[49] H. Zhang, J. Zhang, *J. Colloid Interface Sci.* **2020**, *569*, 254.
[50] D. Zhang, W. Zhou, B. Wei, X. Wang, R. Tang, J. Nie, J. Wang, *Carbohydr. Polym.* **2015**, *125*, 189.
[51] Y. Han, Y. Lu, *Carbon* **2007**, *45*, 2394.
[52] S. N. Alam, N. Sharma, L. Kumar, *Graphene* **2017**, *6*, 1.
[53] X. Liu, J. Liu, S. Lin, X. Zhao, *Mater. Today* **2020**, *36*, 102.
[54] G. Cai, J. Wang, K. Qian, J. Chen, S. Li, P. S. Lee, *Adv. Sci.* **2017**, *4*, 1600190.
[55] H. Sun, Y. Zhao, S. Jiao, C. Wang, Y. Jia, K. Dai, G. Zheng, C. Liu, P. Wan, C. Shen, *Adv. Funct. Mater.* **2021**, *31*, 2101696.
[56] J. Cao, Z. Zhang, K. Li, C. Ma, W. Zhou, T. Lin, J. Xu, X. Liu, *Nanomaterials* **2023**, *13*, 2465.